

AVOID-JACK: Avoidance of Jackknifing for Swarms of Long Heavy Articulated Vehicles

Adrian Schönagel^{1,2}, Michael Dubé¹, Christoph Steup², Felix Keppler² and Sanaz Mostaghim^{1,2}

Abstract—This paper presents a novel approach to avoiding jackknifing and mutual collisions in Heavy Articulated Vehicles (HAVs) by leveraging decentralized swarm intelligence. In contrast to typical swarm robotics research, our robots are elongated and exhibit complex kinematics, introducing unique challenges. Despite its relevance to real-world applications such as logistics automation, remote mining, airport baggage transport, and agricultural operations, this problem has not been addressed in the existing literature.

To tackle this new class of swarm robotics problems, we propose a purely reaction-based, decentralized swarm intelligence strategy tailored to automate elongated, articulated vehicles. The method presented in this paper prioritizes jackknifing avoidance and establishes a foundation for mutual collision avoidance. We validate our approach through extensive simulation experiments and provide a comprehensive analysis of its performance. For the experiments with a single HAV, we observe that for 99.8 % jackknifing was successfully avoided and that 86.7 % and 83.4 % reach their first and second goals, respectively. With two HAVs interacting, we observe 98.9 %, 79.4 %, and 65.1 %, respectively, while 99.7 % of the HAVs do not experience mutual collisions.

I. INTRODUCTION

Distilling complex global swarm behaviors into simple, local rules for individuals is a fascinating challenge [1]. This challenge is especially pronounced in swarm robotics, where robots, unlike biological organisms, are engineered to fulfill human-defined objectives. Swarm robotics has proven effective at a diverse range of tasks, enabling robot swarms to achieve collective goals through interactions governed by these local rules [1].

In most models, robots are approximated as point masses subject to basic kinematic equations (cf. [1], [2]). Common examples include spherical agents, differential-drive vehicles, and aerial drones. Methods for coordinating their motion, whether forming swarm patterns, navigating to target locations, or collaborating on tasks, are widely documented [2].

In [3], we introduced a new challenge: swarms of long, Heavy Articulated Vehicles (HAVs). Two novel subproblems emerge in this context: avoiding infeasible articulation states (i.e., *jackknifing*) and space-efficient mutual collision avoidance. Solving these problems could unlock applications in decentralized conflict resolution for logistics and remote

mining operations, as well as agricultural tasks such as crop harvesting or combined soil preparation and seeding, and scenarios that could use Automated Ground Vehicles (AGVs) with trailers, such as airport baggage transport and factory automation. In this paper, we focus on avoiding jackknifing in HAVs by introducing a novel attraction-repulsion-based swarm behavior referred to as *AVOID-JACK*. Section III details the problem formulation.

II. STATE OF THE ART

The literature on multi-robot systems is divided into centralized and decentralized approaches. Centralized methods for robots with simple kinematics are well established and extensively studied [4], [5]. However, research addressing robots with complex kinematics, such as HAVs, is much more limited. Some works have explored centralized coordination of trajectories for these platforms [6], and a few have considered dynamic rescheduling in response to disturbances [7]. Local path planning for such vehicles has been studied [8] but is not yet fully integrated into multi-robot systems.

On the decentralized side, the field of swarm robotics has focused on robots with simple kinematic models [1], [2], [9]. There have been some extensions to non-holonomic systems, such as cars [10] and fixed-wing aircraft [11], among others. While these studies incorporate movement constraints, they often rely on simplified collision avoidance strategies and do not fully capture more complex kinematic behaviors.

Some work exists in the area of distributed model predictive control (MPC), but these either focus on trucks

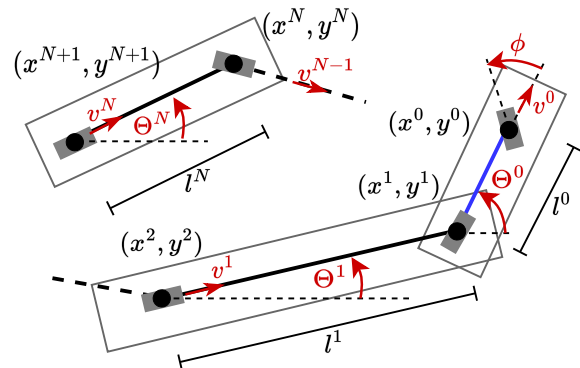


Fig. 1. Ackermann Truck-Trailer Model for HAV i . The truck (blue) and first trailer (black) are shown at the bottom right, while the final trailer N_i is depicted at the top left. Intermediate trailers are omitted and indicated by a thick dashed line. For simplicity, the subscript i is omitted from the variables.

This research was funded by EFRE Saxony-Anhalt, grant number ZS/2023/12/182177, and supported by the Fraunhofer Internal Programs under Grant No. Attract 40-11882.

¹ Chair for Computational Intelligence, Otto-von-Guericke-University, Magdeburg, Germany {adrian.schoennagel, michael.dube, sanaz.mostaghim}@ovgu.de

² Fraunhofer Institute for Transportation and Infrastructure Systems IVI, Dresden, Germany {christoph.steup, felix.keppler}@ivi.fraunhofer.de

without trailers for arbitrary tasks [12] or handle trailers, but only for very specific tasks such as lane changing [13]. Even less work exists in the area of distributed multi-robot systems (MRS) control, focusing on very specific use cases such as leader-follower behavior [14].

To the best of our knowledge, fully decentralized approaches for multi-robot systems with complex kinematics remain an open research area and are the focus of this study.

III. PROBLEM DESCRIPTION

In decentralized swarms of long HAVs — each comprising an Ackermann-steered truck towing one or more passive trailers — the two major challenges are avoiding jackknifing and efficient mutual collision avoidance [3]. These challenges persist regardless of the swarm’s specific objectives.

Section III-A details our vehicle assumptions and kinematic model. Sections III-B and III-C examine the jackknifing and collision avoidance problems, respectively. Finally, Section III-D describes the scenario studied in this paper.

A. KINEMATIC MODEL

We model each HAV i as a truck pulling N_i trailers, assuming negligible width, on-axle hitching, and length equal to wheelbase for each segment. Let a *virtual-axle* denote the centroid of all corresponding physical axles. Then, let the truck’s front and rear virtual-axles be indexed by $k = 0, 1$, respectively, and each trailer $j \in [1, N_i] \subset \mathbb{N}$ have a single rear virtual-axle indexed by $k = j + 1$. Let (x_i^k, y_i^k) denote the position of the k^{th} virtual-axle and let Θ_i^0, Θ_i^j be the heading of the truck and trailer j , respectively. The truck’s and j^{th} trailer’s wheelbases are l_i^0 and l_i^j , respectively. A schematic of HAV i with N_i trailers is shown in Fig. 1.

Each HAV is controllable through the velocity $v_i^0 \geq 0$ and steering angle $\phi_i \in [-\phi_i^{\max}, \phi_i^{\max}]$ of the truck. Where v_i^0 is the truck’s speed, Θ_i^0 is its direction, and v_i^j is the j^{th} trailer’s speed. With the nomenclature and on-axle hitching simplification, we adapt the differential equations from [15], provided in (1) and (2).

$$\begin{pmatrix} \dot{x}_i^1 \\ \dot{y}_i^1 \\ \dot{\Theta}_i^0 \end{pmatrix} = \begin{pmatrix} v_i^0 \cdot \cos(\Theta_i^0) \\ v_i^0 \cdot \sin(\Theta_i^0) \\ v_i^0 / l_i^0 \cdot \tan(\phi_i) \end{pmatrix} \quad (1)$$

$$\forall j \in [1, N_i]: \begin{pmatrix} \dot{\Theta}_i^j \\ v_i^j \end{pmatrix} = \begin{pmatrix} -\frac{v_i^{j-1}}{l_i^{j-1}} \cdot \sin(\Theta_i^j - \Theta_i^{j-1}) \\ v_i^{j-1} \cdot \cos(\Theta_i^j - \Theta_i^{j-1}) \end{pmatrix} \quad (2)$$

B. JACKKNIFING

Jackknifing occurs when the angle between two consecutive segments exceed a maximum articulation angle, leading to severe damage to the vehicle. We denote the articulation angle between trailer j and its preceding segment as $\delta_i^j = \Theta_i^j - \Theta_i^{j-1}$ for $j = 1, \dots, N_i$. Through trigonometric relationships, the inequality constraints (3) become (4). Although we set this angle limit to 90° ($\pi/2$ radians), the equations work for any angle $\in (0, \pi]$.

$$\forall j \in [1, N_i]: \quad \pi/2 \geq \left| \delta_i^j \right| \quad (3)$$

$$\forall j \in [1, N_i]: \quad 0 \leq \cos(\delta_i^j) \quad (4)$$

C. MUTUAL COLLISION AVOIDANCE

HAV i can be approximated as a circle around the truck with center (x_i^1, y_i^1) and *collision radius* $d_i = \sum_{j=1}^{N_i} l_i^j$ (the *footprint*). Then the *collision distance* of HAV i and h is $d_{i,h} = d_i + d_h$. They are in *potential collision* if their circles overlap, that is (5) holds. For a more exact version, consider P_i to be a polygonal chain connecting the axles of HAV i . If the polygonal chain of HAVs i and h intersect, they are considered to be in *actual collision* (i.e., (6) holds).

$$\|(x_i^1, y_i^1)^T - (x_h^1, y_h^1)^T\|_2 \leq d_{i,h} \quad (5)$$

$$P_i \cap P_h \neq \emptyset \quad (6)$$

D. SCENARIO

Let there be M HAVs in a 2D space with no known obstacles. Each HAV i starts from a *start pose* $\mathcal{P}_i^S = \{p_{x,i}^S, p_{y,i}^S, p_{\Theta,i}^S\}$ such that its truck’s rear axle (x_i^1, y_i^1) and heading Θ_i^0 are assigned these values, and its trailers have no articulation. It is then assigned consecutive *goal poses* $\mathcal{P}_i^G = \{p_{x,i}^G, p_{y,i}^G, p_{\Theta,i}^G\}$ for the same axle. In these, trailer articulation is not restricted except for jackknifing; see (4).

The start and goal poses for all HAVs are chosen such that they are not in potential collision; that is, there is no pair $(i, h) \in \{1, \dots, M\}^2, i \neq h$ for which (5) holds.

IV. AVOID-JACK

Let a vector $\vec{m}_i = (m_i^x, m_i^y)^T$ define the desired movement of HAV i . Then, one can translate \vec{m}_i into the Ackerman control commands v_i^0 and ϕ_i by (7) and (8); see Fig. 2. Note that ϕ_i is clipped into the HAVs’ steering limits $[-\phi_i^{\max}, \phi_i^{\max}]$.

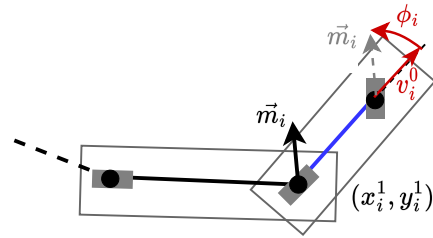


Fig. 2. Translation of Vector to Ackermann Movement.

$$v_i^0 = \|\vec{m}_i\|_2 \quad (7)$$

$$\phi_i = \arctan(m_i^x, m_i^y) - \Theta_i^0 \quad (8)$$

s.t. $\phi_i \in [-\phi_i^{\max}, \phi_i^{\max}]$

With this notation, attractive and repulsive forces on the vehicle are modeled as independent vectors and then combined into a total movement vector. Given the segment lengths l_i^j and (1) and (2), the next vehicle state $\mathcal{S}_i = \{x_i^k, y_i^k, \Theta_i^0, \dots, \Theta_i^{N_i}\}$ follows. All axle positions (x_i^k, y_i^k) can then be obtained via trigonometry if needed.

In the remainder of this section, we propose a method to model jackknife avoidance, goal attraction, and mutual collision avoidance via such attractive and repulsive vectors.

A. JACKKNIFE AVOIDANCE

Our jackknife avoidance strategy models alignment of the truck-trailers through repulsion forces, which increase with articulation. This is possible because the truck and its trailers are not individuals but are tied together, which translates tugging forces of the truck on the trailers to alignment changes. Our approach is presented in Theorem 1 and Solution 1 and then proven given Assumptions 1 and 2.

Assumption 1. *When an HAV is almost straight, a low or zero steering angle will make it straighter.*

Assumption 2. *Aligning the truck with its first trailer and then continuing straight ahead will reduce articulation in all trailers in the long term. Although the articulation could increase in rearward joints for a short time horizon Δ_T it will decrease thereafter; cf. (9).*

$$\exists \Delta_T \geq 0 : \forall t \geq 0, j : |\delta_i^j(t_0 + \Delta_T + t)| \leq |\delta_i^j(t_0)| \quad (9)$$

Theorem 1. *A properly designed behavior consisting of a weight function $w^{\text{jack}}(\delta)$ combining repulsion $(\cos \Theta_i^1, \sin \Theta_i^1)^T$ and goal attraction \vec{m}_i^G will repel the HAV from non-recoverable articulation states.*

Solution 1 (to Theorem 1). *The weight function $w^{\text{jack}}(\delta)$ is designed as the activation of the articulation angle repulsion; see (15) and Fig. 3. The weight is then calculated for each joint of the HAV, summed, and multiplied with the direction induced by the heading Θ_i^1 of the first trailer; see (10). Given any goal heading vector \vec{m}_i^g with length $\|\vec{m}_i^g\|_2 = 1$, one can obtain the total movement vector \vec{m}_i through (10) by (11).*

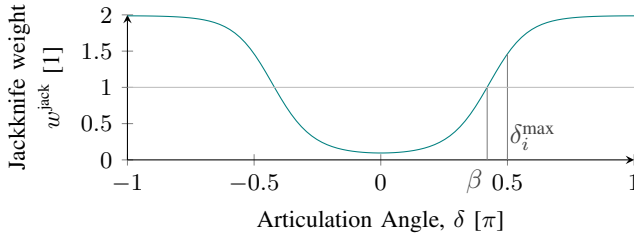


Fig. 3. Function for Jackknife Weight over Articulation Angle, see (15).

$$\vec{u}_i = \vec{m}_i^g + \left[\sum_{j=1}^{N_i} w^{\text{jack}}(\delta_i^j) \right] \cdot \begin{pmatrix} \cos \Theta_i^1 \\ \sin \Theta_i^1 \end{pmatrix} \quad (10)$$

$$\vec{m}_i = v_i^{\text{max}} \cdot \frac{\vec{u}_i}{\|\vec{u}_i\|_2} \quad (11)$$

Proof of Theorem 1 using Solution 1. Starting from the straight start pose \mathcal{P}_i^S , it is obvious that with $\phi_i \rightarrow 0$ all $|\delta_i^j|$ will decrease, and that with $|\phi_i| \rightarrow \phi_i^{\text{max}}$ articulation will increase the most. Then, the articulation of the first trailer will increase more than that of consecutive trailers. That is $\forall j : \delta_i^1 \geq \delta_i^j$ since $v_i^0 \geq v_i^j$; see (2).

Through the design of $w^{\text{jack}}(\delta)$ one can choose $\beta < \delta_i^{\text{max}}$. Through case distinction, we show stability when starting from a straight HAV:

- If $|\delta_i^1| > \beta$ then $w_i^{\text{jack}} > 1$. Therefore, all δ_i^j will decrease in absolute value in the next step.
- If $|\delta_i^1| = \beta$ then $|\Delta \delta_i^1| < \delta_i^{\text{max}} - \beta$ must hold in Δt in order to not jackknife. Combining $\delta_i^1 = \Theta_i^1 - \Theta_i^0$ with (1) and (2) yields (12):

$$\dot{\delta}_i^1 = -\frac{v_i^0}{l_i^1} \sin(\delta_i^1) - \frac{v_i^0}{l_i^0} \tan(\phi_i) \quad (12)$$

Over one time step of Δt the maximum change in δ_i^1 can then be computed through (13) by (14):

$$\begin{aligned} \max |\Delta \delta_i^1| &= \max |\dot{\delta}_i^1| \cdot \Delta t \\ &= v_i^0 \Delta t \cdot \underbrace{\left| \frac{\sin(\delta_i^1)}{l_i^1} + \frac{\tan(\phi_i^{\text{max}})}{l_i^0} \right|}_{\text{constant since } \delta_i^1 = \beta} \end{aligned} \quad (13)$$

Therefore, with well-chosen *reaction distance* $v_i^0 \cdot \Delta t$ and *articulation threshold* β , articulation will not exceed its allowed maximum.

- Finally, if $|\delta_i^1| < \beta$ then $|\Delta \delta_i^1| < \max |\Delta \delta_i^1|$, see (14). \square

We choose $\beta = 75^\circ$ and $\max_\delta(w^{\text{jack}}) = 2$, which leaves us with $b = 0.5$ and $c = 2$ in Eq. (15). From (14), we can then compute $v_i^{\text{max}}(\Delta t, l_i^0, l_i^1)$ as (16).

$$w^{\text{jack}} = 1 + \tanh(b - c \cos(\delta)) \quad (15)$$

$$v_i^{\text{max}} = \frac{\delta_i^{\text{max}} - \beta}{\Delta t \cdot \left| \frac{\sin(\beta)}{l_i^1} + \frac{\tan(\phi_i^{\text{max}})}{l_i^0} \right|} \quad (16)$$

To validate the applicability of the proven strategy, it is critical to assess the correctness of the assumptions. While Assumption 1 is straightforward, Assumption 2 needs to be tested experimentally; see Section VI.

B. GOAL ATTRACTION

Given any current pose $\{x_i^1, y_i^1, \Theta_i^0\}$ and goal pose \mathcal{P}_i^G , one can compute a connecting Dubins path [16] consisting of a concatenation of circles and up to one straight. For the radius of the circles, we choose the radius of the minimal stable circle HAV i can drive on.

Theorem 2. *The minimal stable circle that HAV i can drive on for infinite time has radius R_i^{min} ; computed by (17).*

$$R_i^{\text{min}} = \sqrt{\sum_{j=0}^{N_i} (l_i^j)^2} \quad (17)$$

Proof. In a stable circle, all axles of the HAV rotate around a common instantaneous center of rotation (ICR). This requires that all wheels move along the tangent of their respective circles. That is, their extended axle points towards the ICR. From Fig. 4 we get the relations $R_i^{\text{min}2} = l_i^0^2 + R_i^1^2$, $R_i^1^2 = l_i^1^2 + R_i^2^2$, etc. until only the radius R_i^{N+1} of the last axle's circle remains. Then we see that $R_i^{\text{min}2} = \sum_{j=0}^{N_i} (l_i^j)^2 + R_i^{N+1}^2$. It is trivial to see that R_i^{min} becomes

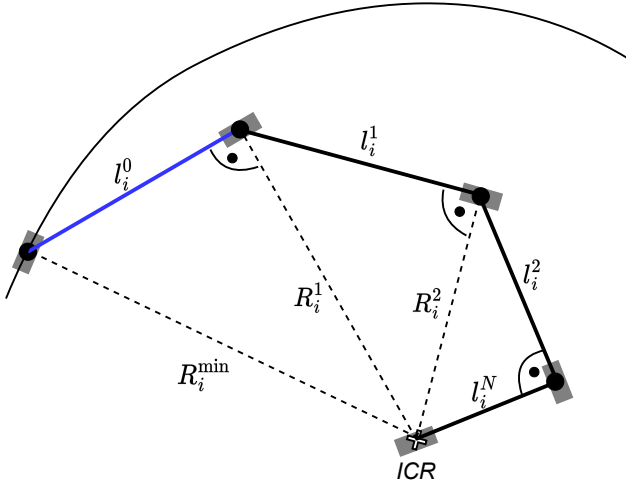


Fig. 4. Minimum stable circle of an example HAV. (blue: truck, black lines: trailers, arc: sub-arc of minimal circle).

minimal when $R_i^{N+1} = 0$, i.e., the last axle is in the ICR, yielding Eq. (17). \square

Note that the stable state might be reached only after multiple rotations of the truck on the circle, depending on starting articulation. Before that, trailer articulation will be smaller. In addition, please note that the stable state is jackknifing-free. Also note that the HAV may transiently drive smaller-radius arcs, depending on trailer configuration and steering limits. The stable circle denotes what is jackknife-safe indefinitely, and thus safe to use in dubins paths.

To improve heading accuracy, we define an *approach point* \mathcal{P}_i^A one truck length before the goal \mathcal{P}_i^G ; see (18). Then the goal heading vector \vec{m}_i^g for HAV i can be computed by Algorithm 1.

$$\mathcal{P}_i^A = \mathcal{P}_i^G - l_i^0 \cdot \begin{pmatrix} \cos p_{\Theta_i^G, i}^G \\ \sin p_{\Theta_i^G, i}^G \end{pmatrix} \quad (18)$$

C. MUTUAL COLLISION AVOIDANCE

For mutual collision avoidance, we use circular approximations as described in Section III-C. If the distance between HAVs i and h falls below their collision threshold $d_{i,h}$, they replace their goal attraction vectors \vec{m}_i^g and \vec{m}_h^g by vectors directed away from each other. Currently, priority is given to the first detected HAV that initiates evasion; cf. (10). Alternative policies are not explored in this paper. This approach can similarly be applied to environmental obstacles detected during execution by modeling them as point masses with a defined collision distance that vehicles must avoid.

V. EXPERIMENT DESIGN

In this paper, we focus our analysis on the bilateral interaction between two swarm members, as the combination of their large state spaces leads to highly complex scenarios. To investigate these interactions, we designed a set of randomized experiments per Section III-D involving one and

Algorithm 1 Goal Attraction

Require: $\mathcal{P}_i^G, \mathcal{P}_i^A, x_i^1, y_i^1, \Theta_i^0, R_i^{\min}$

Ensure: \vec{m}_i^g

if close to goal **then**

$P \leftarrow \mathcal{P}_i^G$

$R \leftarrow l_i^0 \quad \triangleright$ Allow sharper turns when close to goal

else

$P \leftarrow \mathcal{P}_i^A$

$R \leftarrow R_i^{\min}$

end if

Compute Dubins path from current pose to P with R

if dubins path starts with left curve **then**

$\phi \leftarrow +\phi_i^{\max}$

else if dubins path starts with right curve **then**

$\phi \leftarrow -\phi_i^{\max}$

end if

$$\vec{m}_i^g = 1 \cdot \begin{pmatrix} \cos(\Theta_i^0 + \phi) \\ \sin(\Theta_i^0 + \phi) \end{pmatrix}$$

two HAVs. We test two **Hypotheses**: 1) Assumption 2 holds, at least for HAVs with few trailers; 2) HAVs reach their goals. To evaluate Hypothesis 1, we introduce two metrics: the *Joint Position Metric*, locating the joint along the HAV length, and the *Length Difference Metric*, the cumulative trailer-length difference normalized by HAV length.

To model real-world truck-trailer combinations, each HAV i is composed of a single truck and N_i trailers, where $N_i \in \{1, \dots, 10\}$ is sampled from a Rayleigh distribution with $\sigma = 3$ (see Fig. 5). The truck length $l_i^0 \in [2\text{m}, 12\text{m}]$ is sampled from a mixed Gaussian distribution with $\mu_1 = 4\text{m}, \sigma_1 = 0.6, \mu_2 = 10.7\text{m}, \sigma_2 = 1.2$ (see Fig. 6). Each trailer length $l_i^j \in [2\text{m}, 12\text{m}]$ is independently sampled from a uniform distribution.

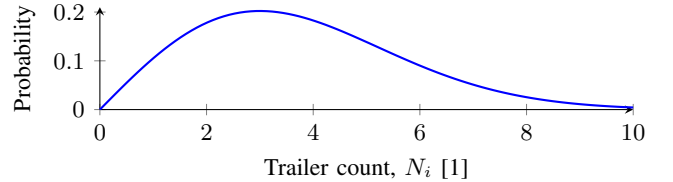


Fig. 5. Trailer Count Distribution.

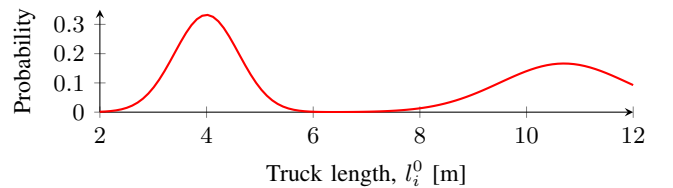


Fig. 6. Truck Length Distribution.

We then sequentially assign a start pose to each HAV. The pose is randomly sampled from a uniform distribution in 2D space plus heading such that $0 \leq x \leq A, 0 \leq y \leq A$ and

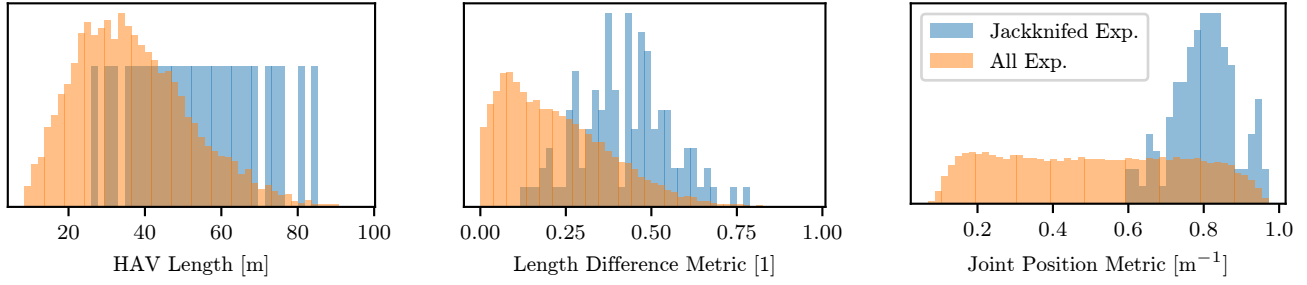


Fig. 7. Probability Distribution of Experimental Results for Two HAV Experiments. Y-axis scaled differently between subplots for maximum clarity.

$0 \leq \Theta^0 \leq 2\pi$, where A^2 is the *area size* and $\forall j : \Theta^j = \Theta^0$. If the sampled pose is in potential collision with any previously sampled HAV (see (5)), a new random pose is chosen until a valid pose is found. A is chosen such that the area is equal to quadruple the sum of the area footprint of all HAVs: $A^2 = 4 \cdot \sum_i (\pi d_i^2)$. The first and second goal poses of each HAV are then set following the same schema. Note that, e.g., the first goal poses are restrained with respect to each other, and there are no constraints to other phases.

A goal is determined as reached (hit) when the corresponding HAV’s truck’s rear axle is less than $d_e^G = 0.5$ m away: $\|p_{x,i}^G - x_i^1, p_{y,i}^G - y_i^1\|_2 < d_e^G$ and their heading differs no more than $d_h^G = 0.1$ rad: $|(p_{\Theta,i}^G - \Theta_i^0 + \pi) \bmod 2\pi - \pi| < d_h^G$. The HAV’s maximum velocity is then imitatively reduced to zero. Once every HAV has reached its first goal, all HAVs’ maximum velocities are reset, and they are assigned their second goal. For our chosen parameters, we can observe that $v_i^{\max} \geq 1 \text{ m s}^{-1}$ for $\Delta t = 0.2$ s; see (16). Therefore, we set $v_i^{\max} = 1 \text{ m s}^{-1}$ for all trucks in our simulations. We then simulate 4,500 single-HAV and 4,500 two-HAV experiments. Each experiment runs for a maximum of 20,000 time steps, terminating early only when the second goals are reached by all HAVs in the experiment.

The code used to execute the experiments in simulation and the resulting data are provided through Zenodo¹.

VI. SIMULATED EXPERIMENT RESULTS

This section presents the results of the experiments outlined in Section V. We focus on jackknifing avoidance in Section VI-A, followed by an analysis of goal-reaching performance, reasons for missed goals, and thoughts on mutual collisions in Sections VI-B to VI-D.

A. JACKKNIFING

Out of 4,500 single-HAV experiments, only 7 (0.16%) featured at least one jackknifed pose (i.e., violating (4)). In the 4,500 two-HAV experiments (9,000 HAVs), 95 HAVs (1.1%) experienced jackknifing.

Fig. 7 shows three histograms for the two-HAV experiments, comparing all runs to jackknifing cases. The left histogram reveals that jackknifing is more frequent in longer HAVs, suggesting a positive correlation with vehicle length.

The same trend appears for trailer count, where we didn’t see any jackknifing for HAVs with less than four trailers. The second histogram, using the Length Difference Metric, indicates higher jackknifing likelihood with larger cumulative trailer-length differences, whereas the length difference at the affected joint itself does not correlate. The third histogram, showing the Joint Position Metric, reveals that jackknifing predominantly occurs at the rear joints.

These results partially support Hypothesis 1: While Assumption 2 might not be universally valid, it holds for shorter HAVs, those with fewer trailers, and those with smaller trailer length differences. We also learn that jackknifing occurs more often during HAV interactions, suggesting a link to our mutual collision avoidance strategy.

B. GOAL REACHING PERFORMANCE

We next evaluate the HAVs’ ability to reach their assigned goals. Each HAV had two sequential goals per experiment. In the 4500 single-HAV experiments, 3904 reached the first goal (86.7%), and 3754 the second (83.4%). In the 4500 two-HAV experiments, 7142 trucks reached the first goal (79.4%), and 5856 the second (65.1%).

Fig. 8 presents three histograms for the two-HAV experiments: heading difference at goal achievement, Euclidean distance at goal achievement (most successes 0.3 m–0.5 m, threshold 0.5 m), and time steps to reach each goal.

Further analysis reveals that the probability of goal achievement is independent of initial Euclidean distance, heading difference, and inter-goal distance. HAVs approach goals from a wide range of headings and finish within the allowed distance thresholds. Euclidean distance would reduce in the next simulation step, suggesting heading, not distance, limits goal completion.

Comparing the first and second goals, we find similar distributions in all metrics. Finally, we observe that single- and two-HAV experiments follow comparable trends, though two-HAV success rates are lower, likely due to increased complexity and collision avoidance demands.

These findings support Hypothesis 2, demonstrating that HAVs can generally reach their assigned goals, although the presence of other HAVs can reduce the overall success rate.

C. GOAL MISS ANALYSIS

To better understand why HAVs sometimes fail to reach their goals, we define two types of *close misses*, which ex-

¹Code DOI: 10.5281/zenodo.17342236

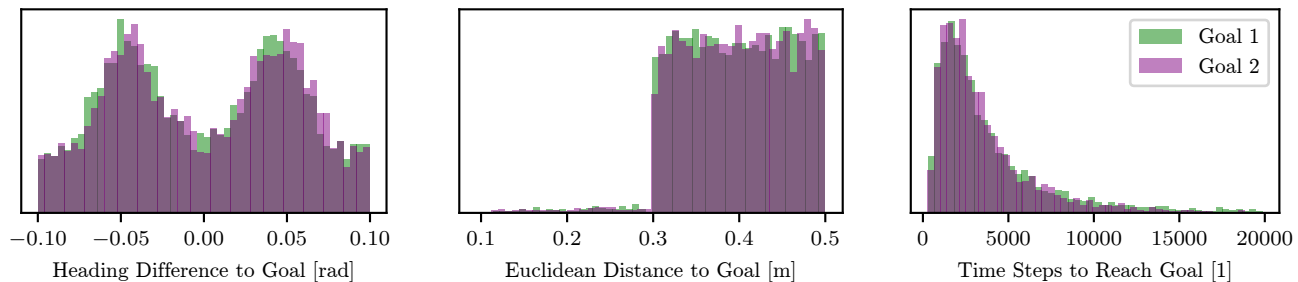


Fig. 8. Probability Distribution on Goal States for Two HAV Experiments. Y-Axis scaled differently between subplots for maximum clarity.

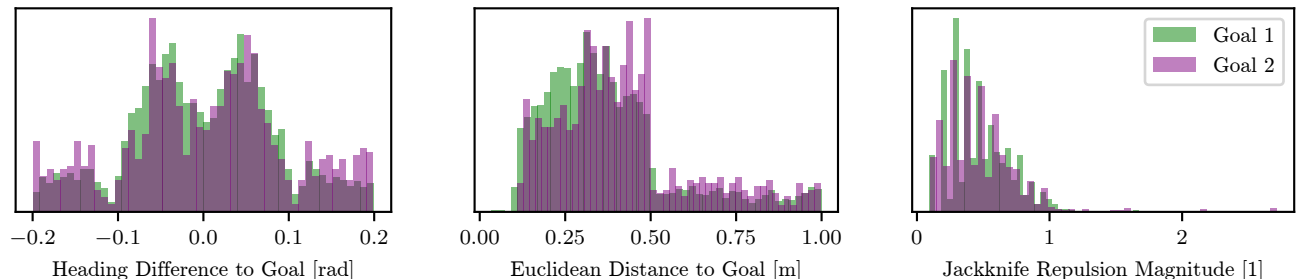


Fig. 9. Probability Distribution on Close Misses for Two HAV Experiments. Y-Axis scaled differently between subplots for maximum clarity.

clude hits. A heading close miss occurs when the Euclidean distance threshold is met and the heading difference is in $[d_h^G, 2d_h^G]$. A Euclidean close miss occurs when the heading difference threshold is met and the Euclidean distance is in $[d_e^G, 2d_e^G]$. Any state where either of the above criteria is true for either of the goals is recorded as a close miss.

In these cases, of the two-HAV experiments, HAVs often experienced active jackknife repulsion; see Fig. 9 rightmost. However, due to static repulsion increasing with trailer count, we cannot conclusively attribute missed goals to jackknife repulsion, though some correlation is likely.

Analysis of the two leftmost histograms in Fig. 9 shows that close misses usually fall within the distance threshold d_e^G , while heading differences are more dispersed. Further investigation shows that heading close misses constitute the majority with 67% and 68% for the first and second goals.

Finally, from the previous subsection we find that two-HAV experiments have significantly more missed goals than single-HAV runs, implying mutual collision avoidance is a key factor. Yet it was inactive during close misses, suggesting earlier activation would have driven the system into a state preventing goal achievement.

D. MUTUAL COLLISIONS

Among the 9000 HAVs in the two-HAV experiments, a potential collision was detected 8.516 times (94.6%), while an actual collision occurred in 26 cases (0.3%). This means that 0.3% of potential collisions resulted in an actual collision. One possible explanation for these actual collisions is the current prioritization of jackknife avoidance over mutual collision avoidance; cf. (10). To further reduce the occurrence

of collisions, additional analysis is needed, including comparisons with more advanced behavior selection mechanisms such as context steering [17].

VII. CONCLUSION AND FUTURE WORK

In this work, we proposed a core mechanism for swarm behavior to reliably automate a fleet of HAVs. We present mechanisms to avoid the main problems of jackknifing and mutual collisions. Jackknifing occurred in 0.2% and 1.1% of single- and two-HAV experiments, respectively, while mutual collision was present in 0.3% of cases. Therefore, *AVOID-JACK* was able to avoid both problems most of the time. Consequently, it provides a baseline for future work and establishes the foundation of this new research field.

In future work, we aim to extend our approach in several key directions. First, we plan to address more challenging environments that feature restricted spaces and known static obstacles. For collision avoidance, we intend to develop more space-efficient footprint approximations and explore methods to combine multiple constraints, such as context steering [17], [18] or sparse roadmap spanners [19]. Improving mutual collision avoidance, particularly in scenarios involving multiple simultaneous potential collisions, remains a priority, as this will allow to scale the approach to larger fleets. Additionally, incorporating hardware experiments with real robots will be essential to validating our methods under real-world conditions, including off-axle hitching. Finally, we plan to account for vehicle-dynamics constraints, such as the inertia of trucks and limited acceleration regarding steering and longitudinal movement, to further improve the realism and applicability of our approach.

REFERENCES

- [1] H. Hamann, *Swarm Robotics: A Formal Approach*. Cham: Springer International Publishing, 2018.
- [2] P. G. F. Dias, M. C. Silva, G. P. Rocha Filho, P. A. Vargas, L. P. Cota, and G. Pessin, "Swarm Robotics: A Perspective on the Latest Reviewed Concepts and Applications," *Sensors*, vol. 21, no. 6, p. 2062, Jan. 2021.
- [3] A. Schönengel, M. Dubé, and S. Mostaghim, "Towards Swarms of Long Heavy Articulated Vehicles," in *GECCO '25 Companion*. Malaga, Spain: ACM, Jul. 2025.
- [4] M. Čáp, P. Novák, A. Kleiner, and M. Selecký, "Prioritized Planning Algorithms for Trajectory Coordination of Multiple Mobile Robots," *IEEE Transactions on Automation Science and Engineering*, vol. 12, no. 3, pp. 835–849, Jul. 2015.
- [5] R. Stern, N. Sturtevant, A. Felner, S. Koenig, H. Ma, T. Walker, J. Li, D. Atzmon, L. Cohen, T. K. Kumar, R. Barták, and E. Boyarski, "Multi-Agent Pathfinding: Definitions, Variants, and Benchmarks," *Proceedings of the International Symposium on Combinatorial Search*, vol. 10, no. 1, pp. 151–158, 2019.
- [6] F. Keppler and S. Wagner, "Prioritized Multi-Robot Velocity Planning for Trajectory Coordination of Arbitrarily Complex Vehicle Structures," in *2020 IEEE/SICE International Symposium on System Integration (SII)*, Jan. 2020, pp. 1075–1080.
- [7] J. Schäfer, F. Keppler, S. Wagner, and K. Janschek, "RMTRUCK: Deadlock-Free Execution of Multi-Robot Plans Under Delaying Disturbances," in *2023 IEEE 26th International Conference on Intelligent Transportation Systems (ITSC)*, Sep. 2023, pp. 1122–1127.
- [8] D. Elueme and Y. He, "A Review of Motion-Planning Methods for Autonomous Articulated Heavy Vehicles," in *Proceedings of the Canadian Society for Mechanical Engineering International Congress*, May 2024.
- [9] A. P. Engelbrecht, *Fundamentals of Computational Swarm Intelligence*. Hoboken, NJ, USA: John Wiley & Sons, Inc., 2006.
- [10] S. A. Kumar, J. Vanualailai, and B. Sharma, "Lyapunov-Based Control for a Swarm of Planar Nonholonomic Vehicles," *Math.Comput.Sci.*, vol. 9, no. 4, pp. 461–475, Dec. 2015.
- [11] S. Hauert, S. Leven, M. Varga, F. Ruini, A. Cangelosi, J.-C. Zufferey, and D. Floreano, "Reynolds flocking in reality with fixed-wing robots: Communication range vs. maximum turning rate," in *2011 IEEE/RSJ International Conference on Intelligent Robots and Systems*, Sep. 2011, pp. 5015–5020.
- [12] L. Dai, Y. Hao, H. Xie, Z. Sun, and Y. Xia, "Distributed robust MPC for nonholonomic robots with obstacle and collision avoidance," *Control Theory and Technology*, vol. 20, pp. 32–45, 2022.
- [13] B. Lourenço and D. Silvestre, "Enhancing truck platooning efficiency and safety—A distributed Model Predictive Control approach for lane-changing manoeuvres," *Control Engineering Practice*, vol. 154, p. 106153, 2025.
- [14] Z. Jin, C. Wang, D. Liang, S. Wang, and Z. Ding, "Fixed-time consensus for multiple tractor-trailer vehicles with dynamics control: A distributed internal model approach," *IEEE Transactions on Intelligent Vehicles*, vol. 9, no. 1, pp. 656–669, 2024.
- [15] O. Sordalen, "Conversion of the kinematics of a car with n trailers into a chained form," in *[1993] Proceedings IEEE International Conference on Robotics and Automation*, May 1993, pp. 382–387 vol.1.
- [16] L. E. Dubins, "On Curves of Minimal Length with a Constraint on Average Curvature, and with Prescribed Initial and Terminal Positions and Tangents," *American Journal of Mathematics*, vol. 79, no. 3, pp. 497–516, 1957.
- [17] A. Fray, "Context Steering: Behavior-Driven Steering at the Macro Scale," in *Game AI Pro 360: Guide to Movement and Pathfinding*. CRC Press, 2019.
- [18] A. Dockhorn, M. Kirst, S. Mostaghim, M. Wiczorek, and H. Zille, "Evolutionary Algorithm for Parameter Optimization of Context-Steering Agents," *IEEE Transactions on Games*, vol. 15, no. 1, pp. 26–35, Mar. 2023.
- [19] W. Hönig, J. A. Preiss, T. K. S. Kumar, G. S. Sukhatme, and N. Ayanian, "Trajectory Planning for Quadrotor Swarms," *IEEE Transactions on Robotics*, vol. 34, no. 4, pp. 856–869, Aug. 2018.